

# Chapter 2

## Theoretical Background and Physical Principles of EHD Instabilities

### 2.1 Fundamental Concepts of Polymers

The availability of materials has been of a considerable impact on the human development over many centuries. Ever since the Stone age, through the Bronze and Iron ages and to the current age emerging as a “Polymer age”, humans have been constantly surrounded by polymers wherever they might be. The naturally occurring biopolymers, the DNA, the proteins and starches in foods, the tires on our bikes and cars, cotton, wool and rubber, are only a number of examples of polymers, which are supreme in their diversity and properties.

A *polymer* is a chemical structure formed by *polymerization*, the process by which elementary units, *monomers* are covalently bonded together. The name is derived from the Greek, (πολυ, polu)-(many) and (μερος, meros)-(parts) and refers to molecules consisting of many repeating monomers. If all the monomer segments are the same, it is called a *homopolymer*, if different, a *copolymer*. The total numbers of structural units,  $N$ , is the *degree of polymerization*. Typically, the outcome of the polymerization process is a mixture of macromolecules with a range of molecular weights,  $M_w$  or *polydispersity* which is one of the distinguishing features of most synthetic polymers and is described by its *molecular weight distribution*. The molecular weight of monomer units,  $M_i$  is typically on the order of 100 while the total weight  $M_{wi} = N_i M_i$  can range from 1,000 to above  $10^6$ . The conventional way to describe the molar mass of a polymer chain is the mass of one mole (equal to Avogadro’s number) of these molecules. The most common units of molar mass are  $g/mol$ , since, in those units the numerical value (i.e., average molecular weight multiplied by Avogadro’s number) equals to the average molecular mass in atomic mass units. The weight distribution is given by the ratio of the total weight of the polymer to the number of molecules and is described by the *number average molecular weight*,  $\bar{M}_n$

$$\bar{M}_n = \frac{\sum_{i=1}^{\infty} M_{wi}}{\sum_{i=1}^{\infty} N_i} \quad (2.1)$$

where  $N_i$  is the number of chains with mass  $M_i$ . The *average molecular weight* where  $M_w$  obtained by randomly choosing the monomer is

$$\bar{M}_w = \frac{\sum_{i=1}^{\infty} M_{wi} M_i}{\sum_{i=1}^{\infty} M_{wi}} = \frac{\sum_{i=1}^{\infty} M_i^2 N_i}{\sum_{i=1}^{\infty} M_i N_i} \quad (2.2)$$

The summation  $\sum_{i=1}^{\infty}$  is a notation for a sum over all possible values of structural units where  $i = N$ . The polydispersity index,  $P_d$  is defined as the ratio of the weight- to number average molecular weights  $M_w/M_n$  and is equal to unity for monodisperse polymers. A larger value of  $P_d$  corresponds to polymers with broader molecular weight distribution.

The physical properties of polymeric systems vary and mainly depend on microscopic structure, which is the arrangement of molecules in the bulk. Polymers can exhibit a randomly arranged *amorphous* structure with no order, or a semicrystalline structure with partial organization in ordered *crystalline* regions, called lamellae. In lamellar part of the chains are packed parallel in a crystalline structure, coexisting with amorphous regions between these lamellae. On larger length scales this layered morphology is organised in spherical regions, the spherulites (Fig. 2.1).

*Polymer solutions* are obtained by dissolving a polymer in a solvent. In solution polymer chains can adopt number of configurations depending on the interaction with the solvent. If these are weak the polymer assumes the shape of a random coil with a Gaussian density distribution. At high enough concentrations parts of the coils interpenetrate since the chain cannot distinguish between a neighbor and itself. An important measure of the spatial extent of the coil is its *radius of gyration*,  $R_g$

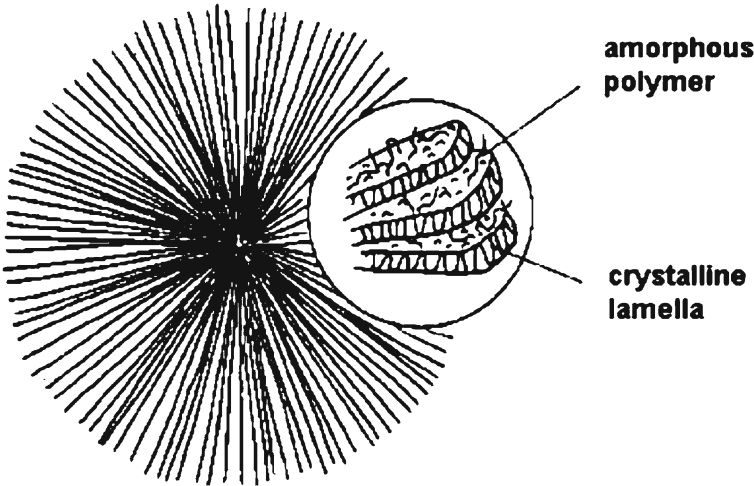


**Fig. 2.1** Crystallization of polymer melts yields semicrystalline materials comprised of folded chains in lamellae which are packed into a larger spherulitic structure, while coexisting with amorphous regions

$$R_g = \frac{l\sqrt{N}}{\sqrt{6}} = \frac{l\sqrt{M_w/M_i}}{\sqrt{6}} \quad (2.3)$$

where  $l$  is the effective segment length.

A bulk liquid state of a *polymer melt* is formed at high enough temperatures when no solvent is present. In the melt, depending on their intermolecular interactions, polymers can be categorized as glassy, semicrystalline, elastic, or viscous. The viscous state, consists of a liquid of macromolecules that are free to move. When this motion is hindered by the presence of cross-links, polymers can only rearrange on length scales smaller than the mean distance between cross-links, and the material is therefore, elastic. Upon cooling, the polymer melt can either transform into a semicrystalline solid below its melting temperature,  $T_m$ , or into a polymeric glass below its glass transition temperature,  $T_g$ . A first order phase transition,  $T_m$  defines the transition from the liquid to crystalline phase and is characterized by discontinuities in the heat capacity and specific volume. While isotactic homopolymers with regular configurations crystallize readily, atactic polymers with random stereochemistry possess some intrinsic disorder that prevents crystallization, and thus, upon cooling (below the polymers'  $T_g$ ) transform into a more brittle amorphous glassy state. In most of the experiments described herein, polymers are in their glassy state at room temperature. At temperatures above their  $T_g$  the segments of the chains become free to move and polymers can be described as incompressible viscous fluids. At the transition temperature from melt to glass, the specific volume varies non-linearly with temperature, but, unlike crystallization, it is continuous. Even though upon cooling or heating through the glass transition range, the material exhibits considerable changes in physical properties, including a change in a heat capacity, there is no latent heat involved. The nature of the glass transition is a subject of continuing research.

Liquid polymers, in comparison to low molecular weight molecules, have a much higher viscosity. Low molecular liquids are often Newtonian fluids with constant viscosities as a function of the flow rate. The viscosity of polymer melts and concentrated solutions is non-Newtonian as it does not show the linear behavior. In the experiments described in this thesis, the melt viscosity  $\eta$  is taken in the limit of zero-shear, or no flow velocity:  $\eta = \eta_0$ . The zero-shear melt viscosity scales linearly with the molecular weight below the entanglement molecular weight,  $M_e$ , where the polymer forms a temporary network of entangled chains. The zero-shear melt viscosity scales with  $M_w$  as  $\eta \propto M_w^{3.4}$ .

Polymeric liquids have a microstructure which resembles springs representing the linear chain. However, polymeric fluids are not ideal elastic materials, and they also have a dissipative reaction to deformation, the viscous dissipation. Thus, at the one end of the frequency spectrum polymeric liquids behave according to Newtonian fluids mechanics, and on the other, according to Hookean elasticity. The viscoelastic (non-Newtonian) behaviour is inherent to all polymers and can be understood in terms of the reptation model. One can easily pull on the end of one polymer coil and it leaves behind a tube, defining the only direction along which the polymer is free to reptate. The time necessary for the molecule to leave this tube defines the reptation time  $\tau_{rep}$ . While for times longer than  $\tau_{rep}$ , the polymer has lost its memory of the

constraining tube and is free to move in any direction, for times shorter than  $\tau_{\text{rep}}$ , the chain is confined to the tube under the influence of Brownian motion, and can only respond elastically.

## 2.2 Stability of Thin Homogeneous Polymer Films

The fundamental understanding along with an ability to fine-tune the physical properties and behavior of thin polymer films are indispensable for a large number of applications in research and industry.

Usually, instabilities in thin films are undesirable in technology. Defect-free smooth films in the form of insulating layers or photoresists, coatings, lubricants or protective layers are essential for most important applications and in particular, in the microelectronics. The practical importance of stable homogeneous films for a variety of technological applications along with the scientific interest in the interactions of liquids near surfaces, have driven the effort to understand the stability of thin liquid films. The dynamics of liquid films have therefore been the subject of many theoretical [1–3] and applied studies [4–8]. A typical thin film is a liquid layer on a substrate with a (free) surface where the liquid is exposed to air (or a gas) or another fluid. Film deposition techniques, such as spin-coating, dip coating or vapor deposition, are used to prepare a thin film on a substrate. Thin polymer films supported on solids substrates exhibit a different behavior relative to both the bulk and the thick films (i.e., films that are thicker than the capillary length). The possibility of an ideal bulk configuration is hindered by the confinement of the polymer chains at the film interfaces. In a confined medium, a film is essentially 2-dimensional, and is different from the bulk. New effects related to the geometry may arise. When the polymer film is laterally confined, it adjusts to the imposed boundary conditions. Liquids in a confined geometry behave differently from those in large volumes. This is due to the dominance of the liquids surface and interfacial tension over other body and surface forces at length scales below the capillary length. In the capillary regime, liquid morphologies are dominated by a minimization of the overall surface free energy. A second aspect where the confinement of a liquid plays a role concerns the stability of thin films. While planar liquid films are intrinsically stable, they can for instance be destabilized by a van der Waals pressure. In the process of film destabilization, the driving force couples to the spectrum of capillary waves and a single capillary mode with a well-defined wavelength develops.

The stability of a thin film is determined by the transient behavior of undulations on its surface. Liquid surfaces are never completely flat. A spectrum of capillary waves is always present caused by the Brownian motion of the molecules. If additional forces couple to this initial capillary wave spectrum, fluctuations might either be amplified or damped. Interactions such as gravity, surface-tension forces, van der Waals forces, externally applied forces such as electric or magnetic fields or temperature gradients acting on the interface yield stresses at the interface and generate film instabilities. The precise control of instabilities in films can however, be utilized to produce novel

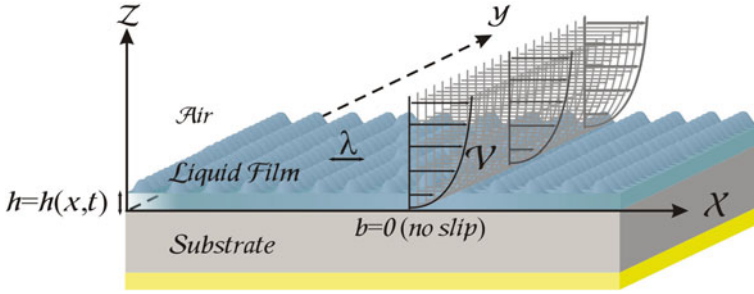


**Fig. 2.2** Schematic representation of a thin supported polymer film with thickness  $h$ . Temperature fluctuations induces capillary surface waves with wavelength  $\lambda$ . The Poiseuille-type flow is indicated by a parabolic flow profile with velocity  $v$

structures by exploiting the destabilization of an initially homogeneous layer in a spontaneous structure formation process, at technologically interesting length scales. Since, instabilities externally induced by electrostatic field are the focal point of this study and are extensively covered in the following chapters, it is essential to take a closer look at the process governing dynamic instabilities of thin liquid films to gain more comprehensive understanding of the physical mechanism(s) behind this process.

The generic experimental system is depicted in Fig. 2.2. A thin polymer film (with initial thickness  $h_0$  is deposited onto a silicon substrate and liquified by annealing above its  $T_g$ . The liquid is described as an incompressible (i.e., constant density,  $\rho$ ) viscous fluid (in the zero frequency limit the liquid is Newtonian, i.e. the shear force per unit area is proportional to the local velocity gradient; the proportionality constant is the viscosity,  $\eta$ ) [9]. The thickness of the film  $h$  is commonly much smaller than the lateral extent of the film  $L$ , and as a result, the flow of liquid primarily takes place in the lateral direction (parallel to the substrate). The  $z$ -coordinate of the film surface is given by  $h = h(x, t)$  where  $x$  is the lateral coordinate,  $t$  is the time. A spectrum of capillary waves is formed at the liquid surface due to the molecular motion of the fluid at finite temperatures. Capillary waves are perturbations of the free interface and generate flow in the film which can be described using a hydrodynamic approach. Calculating the evolution of a capillary wave spectrum is based on assuming a sinusoidal fluctuation with wave number  $q = 2\pi/\lambda$  and amplitude  $\zeta$  ( $\zeta \ll h_0$ )

$$h(x, t) - h_0 = \text{Re}\{\zeta e^{iqx + t/\tau}\} \quad (2.4)$$

The *dispersion relation* relates the time constant  $\tau$  to each  $q$  and establishes whether fluctuations with wavelength,  $\lambda$  ( $\lambda \gg h_0$ , the long wavelength limit relative to the initial film thickness  $h_0$ ) are exponentially amplified or suppressed. The modulation of the free interface determines liquid material transport in the plane of the film which is described by the Navier-Stokes equation and which yields the velocity

profile,  $v$  in the film. In combination with an equation of continuity for the system, the hydrodynamics of the interface can be derived.

### 2.2.1 Hydrodynamics

The motion of an incompressible Newtonian fluid with viscosity  $\eta$  is fully described by classical hydrodynamic theory [9] for known external pressure,  $p$  and an average velocity,  $\bar{v}$ . The Navier-Stokes (N-S) equation of motion for an incompressible fluid is based on Newton's second law stating that an infinitesimal volume element moving with the fluid is accelerated by the forces acting on it. Since the thickness of the film is much smaller than the lateral extent of the film and the flow of liquid primarily takes place in the lateral direction, the explicit vector equation for the  $x$  coordinate is given by:

$$\rho \left( \frac{\partial v}{\partial t} \right) + \rho \left[ u \left( \frac{\partial v}{\partial x} \right) + v \left( \frac{\partial v}{\partial y} \right) + w \left( \frac{\partial v}{\partial z} \right) \right] = - \frac{\partial p}{\partial x} + \eta \left( \frac{\partial^2 v}{\partial x^2} + \frac{\partial^2 v}{\partial y^2} + \frac{\partial^2 v}{\partial z^2} \right) + \rho g \quad (2.5)$$

where the velocity components  $u$ ,  $v$ ,  $w$  are the dependent variables to be solved for and  $g$  is the gravitational acceleration.

The left hand side of a N-S equation is a product of fluid acceleration  $\rho(dv/dt)$  and a convective term  $\rho(v \cdot \nabla v)$  which renders the hydrodynamic equation non-linear. The right hand side of the equation is the total force balance that acts on the fluid element. The forces stem from the pressure gradient at the free interface, the viscous force  $\eta \nabla^2 v$  resulting from the momentum transfer from faster to slower moving layers in the fluid and the gravity ( $\rho g$ ). For flow in thin films, the N-S equation can be simplified in the following way:

1. Since the high viscosities of polymer melts result in a low flow velocity, the quadratic terms in Navier-Stokes equation can be neglected:  $u \left( \frac{\partial v}{\partial x} \right) + v \left( \frac{\partial v}{\partial y} \right) + w \left( \frac{\partial v}{\partial z} \right) \rightarrow 0$ .
2. Since the resulting dynamics are slow, the velocity profile can be considered to be always in a quasi-steady-state:  $\rho \left( \frac{\partial v}{\partial t} \right) \rightarrow 0$ .
3. For thin-films with dimensions smaller compared to the capillary constant (i.e.,  $a = \sqrt{2\gamma/g\rho}$ ), gravity does not have an influence on the shape of the interface:  $\rho g \rightarrow 0$ .
4. For  $\lambda \gg h_0$  and  $\zeta \ll h_0$ : it is possible to approximate the flow in the film as steady laminar flow caused by a pressure gradient in the lateral,  $x$ -direction and the velocity gradient which varies only along the  $z$ -axis.

In order to calculate the dominant wavelength of the instabilities, it is sufficient to simplify the equations to only one lateral coordinate. Additionally, the fluctuations have a small amplitude compared to the film thickness. The further analysis is restricted to wavelengths large compared with the depth of the liquid.

The above considerations yield the simplified Navier-Stokes equation along the  $x$  and  $z$  coordinates:

$$0 = -\frac{\partial p}{\partial x} + \eta \left( \frac{\partial^2 v}{\partial z^2} \right) \quad (2.6)$$

$$\left( \frac{\partial^2 v}{\partial z^2} \right) = \frac{1}{\eta} \frac{\partial p}{\partial x} \quad (2.7)$$

$$\frac{\partial p}{\partial z} = 0 \quad (2.8)$$

Since the pressure is constant within the depth of the film (along  $z$ ), the pressure gradient is a function of  $x$  only, meaning that the pressure gradient along  $x$  is constant. Therefore, integration of this differential equation with respect to  $z$  leads to a parabolic velocity profile:

$$v(z) = \frac{1}{2\eta} \left( \frac{\partial p}{\partial x} \right) z^2 + c_1 z + c_2 \quad (2.9)$$

To calculate the velocity, the boundary conditions related to the values of stresses at the substrate–liquid and liquid–air interfaces must be known. At the substrate in the *lubrication approximation* [10] a non-slip boundary condition is typically assumed  $v(z = 0) = 0$ . At the liquid–air interface ( $z = h$ ) the stress within the fluid is counterbalanced by stresses arising from the surfaces forces. In terms of equation of continuity this boundary condition can be expressed as

$$\eta_{\text{liq}} \frac{\partial v_{\text{liq}}}{\partial z} = \eta_{\text{air}} \frac{\partial v_{\text{air}}}{\partial z} \quad (2.10)$$

Since, there are no stresses in the air (gas), the sum of the viscous and the surface stresses is zero, and the stress at the surface vanishes.

$$\eta_{\text{liq}} \frac{\partial v_{\text{liq}}}{\partial z} = 0 = \sigma_{xz} \quad (2.11)$$

Using the boundary conditions:

1. Zero slip:  $v(z = 0) = 0$   $c_2 = 0$ .
2. No-lateral stresses at the film surface:  $v(z = h)$   $\sigma_{xz} = \eta \frac{\partial v}{\partial z} = 0$ .

yields the constants:

1.  $c_1 = -2 \frac{\partial p}{\partial x} y|_{y=h} = 2 \frac{\partial p}{\partial x} h$ .
2.  $c_2 = 0$ , and the velocity profile is obtained:

$$v(z) = \frac{1}{2\eta} \left( \frac{\partial p}{\partial x} \right) y(z - 2h) \quad (2.12)$$

The mean velocity in the film is:

$$\bar{v} = \frac{1}{h} \int_0^h v(z) dz = \frac{h^2}{3\eta} \left( -\frac{\partial p}{\partial x} \right) \quad (2.13)$$

This equation describes a Poiseuille type flow in the liquid film in the presence of a pressure gradient. The minus sign indicates that the flow is in the direction of the decreasing pressure. In the lubrication approximation, for the one dimensional (1D) case the lateral Poiseuille volume flow rate induced in the direction of decreasing pressure through a cross section of the film,  $A$  is obtained:

$$j = A|_{A=h} \cdot \bar{v} = h \cdot \bar{v} = \frac{h^3}{3\eta} \left( -\frac{\partial p}{\partial x} \right) \quad (2.14)$$

To calculate the interface profile an additional *continuity equation* is required which is derived from the mass conservation of a small volume element (fixed in space) within an incompressible flowing fluid. For two plane cross-sections through the film a distance  $dx$  apart, a volume (per unit time)  $(A\bar{v})_x$  passes through one and  $(A\bar{v})_{x+dx}$  through the other, changes by:

$$(A\bar{v})_x - (A\bar{v})_{x+dx} = -\frac{\partial(A\bar{v})}{\partial x} dx \quad (2.15)$$

Then, the change in volume (due to the variation of incompressible fluid level) per unit time through the film can directly be represented by:  $\frac{\partial(\text{volume})}{\partial t} = \frac{\partial A}{\partial t} dx$  which corresponds to  $\frac{\partial A}{\partial t} dx = -\frac{\partial(A\bar{v})}{\partial x} dx$ , yielding the required equation of motion for the 1-dimensional case ( $A = h$  and  $j = A\bar{v}$ ) that includes the volume conservation:

$$\frac{\partial h}{\partial t} dx + \frac{\partial(A\bar{v})}{\partial x} dx = 0 = \frac{\partial h}{\partial t} + \frac{\partial j}{\partial x} \quad (2.16)$$

Following this any change in the height of the film results in a flow in the lateral direction redistributing the fluid from the valleys to the peaks of the undulations. Substitution of the equation of flux into the equation of continuity yields the final form of the *equation of motion* for the film surface:

$$\frac{\partial h}{\partial t} = \frac{\partial}{\partial x} \left[ \frac{h^3}{3\eta} \frac{\partial p}{\partial x} \right] \quad (2.17)$$

### 2.2.2 Interfacial Pressure

The *interfacial pressure* acting at the surface separating the two media must be determined in order to calculate the dynamics of the liquid–air interface. The total

interfacial pressure is uniform across the depth of the film. However, the pressure does depend on the film thickness. It can be written as sum of several contributions:

$$p(h) = p_0 + p_{\text{vdW}}(h) + p_{\text{L}}(h) + p_{\text{ex}}(h) \quad (2.18)$$

where  $p_0$  is the ambient air pressure which is independent of the film thickness for  $h < \text{capillary length}$ . The second term are the van der Waals (vdW) attractive or repulsive intermolecular forces which act between all atoms and molecules.  $p_{\text{L}}(h)$  is the Laplace pressure stemming from the curvature of the interface and  $p_{\text{ex}}(h)$  can be any excess surface pressure which in this thesis is the electrostatic pressure induced by externally applied electric field,  $p_{\text{el}}(h)$  enabling the electrohydrodynamic (EHD) pattern formation process. In the following paragraphs, the vdW, Laplace and excess pressures are each discussed shortly, eventually establishing the most significant contributions to the total interracial pressure during the EHD patterning process.

### Laplace Pressure

A thoroughly investigated instability is related to destabilizing molecular forces. Destabilizing molecular interactions lead to film rupture if these are sufficiently strong to overpower the stabilizing surface tension. The latter opposes film thickness fluctuations in very thin liquid film. The surface tension  $\gamma$  is defined as the excess free energy at the liquid-air interface that stems from the imbalance in the attractive forces experienced by molecules at the surface of the liquid. To minimize the interfacial energy, a geometric shape with the highest possible volume to surface ratio is formed. Surface tension is the direct outcome of the cohesive forces holding the liquid molecules together. Various phenomena such as capillarity, the shapes of macroscopic liquid droplets on surfaces and the contact angle between coalescing soap bubbles arise from the *surface energy*,  $\gamma$  of solids and liquids (for a liquid,  $\gamma$  is usually referred to as its *surface tension*). Surface tension is the free energy change when the surface area of medium is increased by a unit area. A free liquid will always tend to minimize its surface energy by minimizing its surface area.

A curved liquid surface, which locally increases the surface area, generates a restoring pressure difference, i.e., *Laplace pressure* across the interface, which is inversely proportional to the radii of curvature and scales with the surface tension

$$p_1 - p_2 = \gamma_{\text{L}} \left( \frac{1}{R_1} + \frac{1}{R_2} \right) = p_{\text{L}} \quad (2.19)$$

such that the planes defining the radii of curvature,  $R_1$  and  $R_2$  are perpendicular to each other (Fig. 2.3), and are necessary to describe a curved surface in three dimensions. This equation relates the pressure difference (i.e., Laplace pressure) across the interface to the radius of curvature and the surface tension. In the absence of any other pressure, Laplace pressure always stabilizes the film by damping out all perturbations. For the one dimensional case, the radius of curvature is given by  $1/R = -\partial^2 h / \partial x^2$ , yielding:

$$p_{\text{L}} = -\gamma \frac{\partial^2 h}{\partial x^2} \quad (2.20)$$

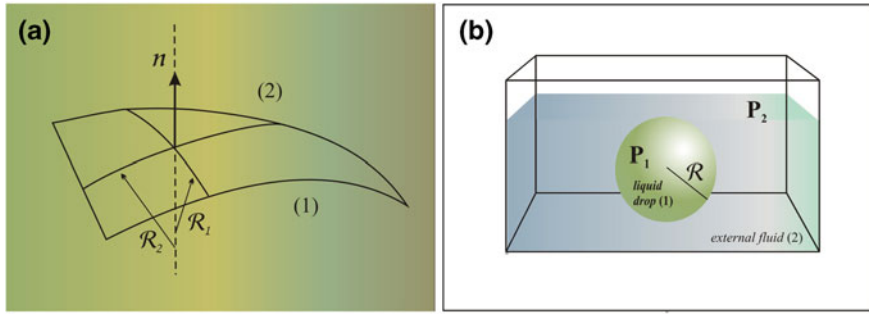


**Fig. 2.3** **a** Illustration of the definition of the principal radii of curvature  $R_1$  and  $R_2$  for a random geometry boundary surface between fluids (1) and (2). **b** Calculation of Laplace pressure: considering a 3D *spherical drop* (1) immersed into a liquid (2), its equilibrium is achieved when the pressure inside the drop,  $P_1$  exceeds the pressure outside  $P_2$  by:  $p_1 - p_2 = p_L = \gamma/R$

For a flat surface the  $R \rightarrow \infty$  and there is no pressure difference across a planar boundary.

### van der Waals Pressure

The stability of very thin ( $h < 10$  nm) liquid films is dictated by the effective molecular interactions between the substrate and the film arising from van der Waals forces. In very thin polymer melt films, vdW interactions are dominant in determining the stability of coatings [8]. These ever present forces, play a role in a host of various phenomena such as surface tension, adhesion and the structure of condensed macromolecules such as proteins and polymers.

Collective, long-range van der Waals forces consist of three important interactions: *Keesom orientation* (i.e., Boltzmann averaged interaction between two permanent dipoles), *Debye induction* (i.e., interaction between a polar and a non-polar molecule) and the *dispersion force* (i.e., interaction between neutral molecules) that together contribute to the total vdW interaction between atoms and molecules. Since, they are always present, independent on the properties of the molecules, dispersion forces also known as induced dipole-induced dipole forces make the most important contribution to the vdW interactions between apolar molecules.

Dispersion forces are quantum-mechanical in origin and amenable to a host of theoretical treatments of varying complexity. Intuitively, they can be understood in terms of an electrostatic interaction arising from the dipole fluctuations of two neighboring atoms or molecules. For a non-polar atom at any given instance, the instantaneous positions of the electrons induce a finite dipole moment which in turn generates an electric field that polarizes neighboring neutral atoms. This induced dipole-induced dipole interaction gives rise to an attractive force between two identical atoms. If two atoms are a substantial distance apart, continuously fluctuating original dipole may have already changed its orientation, and the interaction between them becomes smaller. With distance, this *retardation* effect changes the strength of the van der Waals interaction and its scaling behavior.

For an interatomic vdW pair potential it is possible to sum the energies of all atoms in one body with all the atoms in the other and thus, obtain the “two-body” potential for two surfaces. The resulting interaction is given in terms of the *Hamaker constant*,  $A$ , which quantifies the magnitude of the force and depends on the electronic structure of the involved materials through the density and the strength of the oscillating dipoles. If the Hamaker constant is negative resulting in repulsive van der Waals forces, the film minimizes its free energy by increasing its thickness while wetting the surface and is therefore stable; if the Hamaker constant is positive which means attractive vdW forces, the film reduces its free energy by thinning, and it is unstable and dewets. vdW forces play an eminent role in thin films and the pair-wise integration of all dipole–dipole interactions results in an effective force, which can be either attractive or repulsive depending on the dielectric properties of the film and the bounding materials. The vdW adhesive pressure for the *non-retarded* interaction of a medium 3 sandwiched between two media 1 and 2 is given as

$$p_{\text{vdW}} = -\frac{A_{132}}{6\pi h^3} \quad (2.21)$$

To obtain the Hamaker constant for any system it is essential to know how the dielectric permittivity of every medium varies with frequency, requiring access to the entire electromagnetic frequency spectrum, which is typically not covered by the experimental data. Approximating the Lifshitz calculation, Tabor and Winterton derived a simplified model for calculating the Hamaker constant [11]. However, if the adsorption frequencies of all three media are assumed to be the same, while ignoring molecular rotational frequency,  $\nu_{\text{rot}}$  and considering a main contribution from the electronic UV absorption,  $\nu_e$  ( $\nu_e = 3 \times 10^5 \text{ s}^{-1} \gg \nu_{\text{rot}}$ ), an approximate expression can be obtained for the *non-retarded* Hamaker constant:  $A_{\text{tot}} = A^*_{=0} + A^*_{>0}$

$$A_{\text{tot}} \approx \frac{3}{4}KT \left( \frac{\varepsilon_1 - \varepsilon_3}{\varepsilon_1 + \varepsilon_3} \right) \left( \frac{\varepsilon_2 - \varepsilon_3}{\varepsilon_2 + \varepsilon_3} \right) + \frac{3h_p\nu_e}{8\sqrt{2}} \frac{(n_1^2 - n_3^2)(n_2^2 - n_3^2)}{\sqrt{n_{12} + n_{32}}\sqrt{n_{22} + n_{32}}(\sqrt{n_{12} + n_{32}} + \sqrt{n_{22} + n_{32}})} \quad (2.22)$$

where  $\varepsilon_1$ ,  $\varepsilon_2$  and  $\varepsilon_3$  are the static dielectric constants of the three media,  $n_1$ ,  $n_2$  and  $n_3$  are the corresponding refractive indexes ( $\varepsilon = n^2$ ), and  $h_p$  is Planck’s constant. The first term gives the zero-frequency energy of the vdW interaction and includes the Keesom and Debye dipolar contributions. The second term is the dispersion energy. Since  $h\nu_e \gg kT$ , the dispersive part usually dominates over the dipolar contribution unless the refractive indices of two of the involved materials are similar. The zero-frequency contribution therefore often only accounts for a few percent of the total magnitude of the Hamaker constant. Since it does not depend on the frequency, it is not affected by any retardation. The cross-over from non-retarded to retarded forces occurs typically at film thicknesses on the order of 10 nm, resulting in the vdW force:

$$\Phi_{\text{vdW}} = \frac{B_{132}}{h^4} \quad (2.23)$$

where  $B$  is the retarded Hamaker constant.

### Excess Surface Pressure

$p_{\text{ex}}$  is the energy necessary per unit area to bring two interfaces from infinity to a certain distance  $h$ . It includes any *excess surface pressure*, and is typically called the conjoining pressure  $\Pi$  (the opposite of the *disjoining pressure*).  $\Pi$  is the pressure required to pull the film boundaries, i.e., disjoining them. It is defined as

$$\Pi = -p_{\text{ex}} = -\frac{\partial \Phi}{\partial h} \quad (2.24)$$

where,  $\Phi$  is the excess free energy per unit area, also named *effective interface potential*. The disjoining pressure is usually used for the repulsive interactions in the context of wetting films.

In the absence of any externally applied fields,  $p_{\text{ex}}$  is equivalent to the disjoining pressure caused by the dispersive vdW interactions. For thin films with only non-retarded vdW forces, with the interface potential (adhesion energy)

$$\Phi_{\text{vdW}} = -\frac{A_{132}}{12\pi h^2}. \quad (2.25)$$

When an electric field is externally applied across the liquid polymer-air interface, it polarizes the polymer, it induces an effective surface charge density [12–14]. In this case the dominant external pressure is the destabilising *electrostatic pressure*  $p_{\text{ex}} = p_{\text{el}}$ .

### Electrostatic Pressure

#### Perfect Dielectric

The core of this thesis is the EHD patterning technique which exploits surface instabilities induced by an external electric field. The physical principles of the EHD method are discussed in detail in Sect. 2.3.

The overall pressure distribution at constant temperature in the film for dominant electrostatic interactions is given by

$$p(h) = p_0 + p_L(h) + p_{\text{el}}(h) \quad (2.26)$$

For a sufficiently strong electric field in a capacitor, the electrostatic interactions much stronger than the van der Waals interactions. This means that in electric field experiments the dispersive interactions are only a small correction. Therefore, the vdW pressure can be neglected.

For a perfect dielectric liquid polymer in a capacitor an applied potential difference across the two electrodes (at distance  $d$ ) gives rise to an electric field,  $E_f$  across the dielectric material. The electric field causes the energetically unfavorable build-up

of displacement charges at the dielectric interface, resulting in an effective surface charge density. The charges at the polymer–air interface experience an effective attraction with the oppositely charged upper electrode. Thus, the electric field acts to align the interface separating the two media parallel to the electric field lines while minimizing the free electrostatic energy of the system. The strong electrostatic pressure at the liquid–air interface overcomes the stabilizing effects of the surface tension and destabilizes the film:

$$p_{el} = -\frac{1}{2}\varepsilon_0\varepsilon_p(\varepsilon_p - 1)E_f^2, \quad (2.27)$$

$\varepsilon_p$  is the dielectric constant of the polymer and  $\varepsilon_0$  is the dielectric permittivity of the vacuum. The origin of the destabilizing  $p_{el}$  is schematically shown in Fig. 2.4.  $E_f$  can be calculated from the free energy,  $F$  stored in the capacitor with a constant applied voltage,  $U$

$$F = F_0 - \frac{1}{2}CU^2 \quad (2.28)$$

where  $C$  is the capacitance, and  $F_0$  is the free energy in the absence of an applied voltage. The variation of the free energy with respect to the film thickness,  $h$  per unit area of the interface, gives the interfacial electrostatic pressure

$$p_{el} = \frac{1}{A} \frac{\partial F}{\partial h} = -\frac{U^2}{2A} \frac{\partial C}{\partial h} \quad (2.29)$$

The polymer–air double layer in the capacitor can be modeled as two capacitors in series (Fig. 2.4), one filled with the liquid polymer and the other with air

$$\frac{1}{C} = \frac{1}{C_{\text{dielectric}}} + \frac{1}{C_{\text{air}}} = \frac{d-h}{\varepsilon_0\varepsilon_p A} + \frac{h}{\varepsilon_0\varepsilon_p A} = \frac{\varepsilon_p d - (\varepsilon_p - 1)h}{\varepsilon_0\varepsilon_p A} \quad (2.30)$$

Insertion into Eq. (2.29) for the 1-dimensional case yields

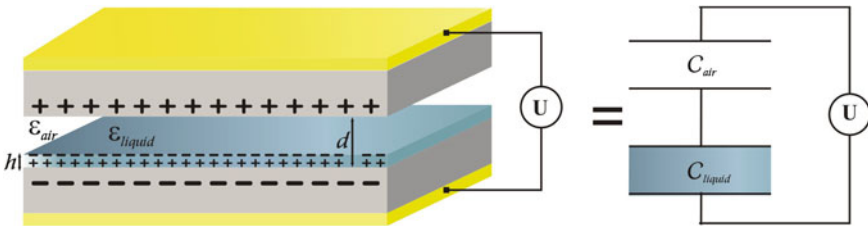


**Fig. 2.4** An applied electric field leads to the polarization of the dielectric polymer layer, yielding an attractive interaction between the charges at the polymer–air interface with the charges at the upper electrode. The layered system is equivalent to a sum of two capacitors in series

$$p_{\text{el}} = -\frac{1}{2} \frac{\varepsilon_0 \varepsilon_p (\varepsilon_p - 1) U^2}{[\varepsilon_p d - (\varepsilon_p - 1)h]^2} \quad (2.31)$$

A comparison with Eq. (2.27), gives the electric field in the polymer

$$E_f = \frac{U^2}{\varepsilon_p d - (\varepsilon_p - 1)h} \quad (2.32)$$

### 2.2.2.1 Leaky Dielectric

In this thesis several materials were subjected to electric field instabilities during the EHD patterning process. While most of the used materials, (i.e., low-viscosity polymers, nanotube-based polymer composite, crystalline polymers and block-copolymers) are well described by a simple linear stability analysis that models the polymer layer as a *perfect dielectric*, for EHD patterning of conductive polymers (Chap. 8), free charges at the interface have to be taken into the consideration. A finite polymer conductivity lowers the electric field in the layer and increases the electrostatic stress at the surface, as predicted in the *leaky dielectric* model by Pease and Russel [15, 16]. The total potential difference spans across the air gap which drives the EHD pattern formation. This is the origin of the instability in the case of a leaky dielectric film.

Similarly to the analysis for the perfect dielectric, the pattern selection of EHD instabilities are given in terms of a linear stability analysis [6, 17] for incompressible, Newtonian fluid assuming the non-slip boundary condition at the substrate. In this case, the destabilising electrostatic pressure is somewhat modified,  $U$

$$p_{\text{el}} = -\frac{1}{2} \frac{\varepsilon_1 \varepsilon_0 U^2}{(d - h_0)^2}. \quad (2.33)$$

### 2.2.3 Linear Stability Analysis and Dispersion Relation

The total interfacial pressure consisting of the destabilizing electrostatic pressure and the stabilizing Laplace pressure,  $p = p_{\text{el}} + \left(-\gamma \frac{\partial^2 h}{\partial x^2}\right)$  couples to the constantly present capillary waves of the liquid surface, which destabilizes part of the mode spectrum. This is described by the well-established *linear stability analysis* of a free liquid film, subjected to a pressure  $p$ , where a sinusoidal form for the film thickness (Eq. 2.4) is used with the temporal evolution of the liquid-air interface governed by equation of motion. Taking the derivative of the equation of motion and inserting the equation for the Laplace pressure gives

$$\begin{aligned}
\frac{\partial h}{\partial t} &= \frac{h^2}{\eta} \left( \frac{\partial h}{\partial x} \right) \left[ \frac{\partial p}{\partial x} \right] + \frac{h^3}{3\eta} \left[ \frac{\partial^2 p}{\partial x^2} \right] \\
&= \frac{h^2}{\eta} \left( \frac{\partial h}{\partial x} \right) \left[ -\gamma \left( \frac{\partial^3 h}{\partial x^3} \right) + \left( \frac{\partial p_{\text{el}}}{\partial h} \right) \left( \frac{\partial h}{\partial x} \right) \right] \\
&\quad + \frac{h^3}{3\eta} \left[ -\gamma \left( \frac{\partial^4 h}{\partial x^4} \right) + \left( \frac{\partial^2 p_{\text{el}}}{\partial h^2} \right) + \left( \frac{\partial p_{\text{el}}}{\partial h} \right) \left( \frac{\partial^2 h}{\partial x^2} \right) \right]. \tag{2.34}
\end{aligned}$$

In the long-wavelength limit, where the amplitude of the surface waves are much smaller than the film thickness ( $\zeta \ll h_0$ ), terms of order  $O(\zeta^2) \ll O(\zeta)$ , where  $\partial h / \partial x \propto \zeta$ , all non-linear terms in  $\zeta$  are discarded simplifying the above equation to

$$\frac{\partial h}{\partial t} = \frac{h^3}{3\eta} \left[ -\gamma \left( \frac{\partial^4 h}{\partial x^4} \right) + \left( \frac{\partial p_{\text{el}}}{\partial h} \right) \left( \frac{\partial^2 h}{\partial x^2} \right) \right] + O(\zeta^2) \tag{2.35}$$

By taking partial derivatives in the above equation and dividing by  $\zeta \exp(iqx + t/\tau)$ , this coupling of a force balance to the capillary wave spectrum yields a *dispersion relation* that describes the temporal evolution of the sinusoidal perturbations in  $h$ :

$$\frac{1}{\tau} = -\frac{h^3}{3\eta} \left[ \gamma q^4 + \frac{\partial p_{\text{el}}}{\partial h} q^2 \right] \tag{2.36}$$

The dispersion relation determines whether a wave with a wave vector  $q$  is damped or amplified. The stability of the film depends on the exact form of the gradient of the excess surface pressure with respect to the film thickness (see Fig. 2.5): while for  $\partial p_{\text{el}} / \partial h \geq 0$ ,  $\tau < 0$  for all  $q$ —fluctuations are damped (due to restoring effect of the surface tension), meaning that all growth rates are negative and the film minimizes its surface and is intrinsically *stable*, for  $\partial p_{\text{el}} / \partial h < 0$  all modes with  $\tau > 0$  and  $q < q_c = \sqrt{-\frac{1}{\gamma} \frac{\partial p_{\text{el}}}{\partial h}}$  are amplified and the film is *unstable*. For  $q > q_c$  undulations are exponentially damped.

The exponentially fastest-growing mode given by the maximum of the dispersion relation eventually dominates the mode spectrum. It has the wavelength  $\lambda = 2\pi/q_{\text{max}}$ :

$$\lambda_{\text{max}} = 2\pi \sqrt{\frac{2\gamma}{-\partial p_{\text{el}} / \partial h}} = 2\pi \sqrt{\frac{\gamma U}{\varepsilon_0 \varepsilon_p (\varepsilon_p - 1)^2}} E_f^{-\frac{3}{2}} = 2\pi \sqrt{\frac{\gamma [\varepsilon_p d - (\varepsilon_p - 1)h]^3}{\varepsilon_0 \varepsilon_p (\varepsilon_p - 1)^2 U^2}} \tag{2.37}$$

The associated maximal growth scales with the fourth power of the dominant wave vector, and is proportional to the ratio of surface tension to viscosity for a given  $\lambda$ :

$$\frac{1}{\tau_{\text{max}}} = \frac{\gamma h^3}{3\eta} q_{\text{max}}^4 \tag{2.38}$$

and

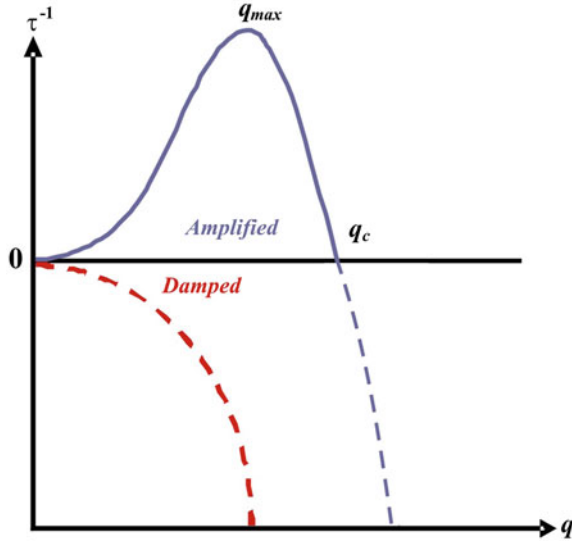


**Fig. 2.5** Graphic representation of the dispersion relation. While in the absence of an electrostatic pressure, all modes are damped ( $\tau < 0$ ), the dispersion relation yields a dominant mode  $q_{\max}$  with a corresponding growth rate  $\tau_{\max}^{-1}$ . In the region of large values of wave vectors ( $\tau < 0$ ), the liquid increases its surface, to an extent that is energetically unfavourable, resulting in suppression of all small wavelength fluctuations. In the region of large wavelength fluctuations ( $\tau > 0$ ), while the waves are exponentially amplified, the growth rate is limited by the viscous dissipation associated with the in-plane transport of material

$$q_{\max} = \sqrt{\frac{-\partial p_{\text{el}}/\partial h}{2\gamma}} = \frac{2\pi}{\lambda_{\max}} \quad (2.39)$$

The two characteristic parameters  $\lambda_{\max}$  and  $\tau_{\max}$  describe the static and dynamic behavior of the liquid film. While the time constant of the EHD instability can provide rheological information, the characteristic wavelength is representative of the forces acting on the polymer–air interface.

## 2.3 Electrohydrodynamic Instabilities in Thin Polymer Films

### 2.3.1 Electrohydrodynamics

Electrohydrodynamics deals with fluid motion induced by electric fields. The physical principles that describe the electrohydrodynamics, which is the deformation of liquid surface induced by an electric field were first noted in 1897 [18], and followed by the original theories on the electrohydrodynamic instabilities [19, 20]. Ever since

these ground-breaking studies, extensive investigation has been carried out on these issues [21–24].

For macroscopic liquid films and liquid jets systems mentioned hitherto, gravity plays an important role. For thin liquid films below the gravity limiting capillary length, electric fields can be used to destabilize the films in order to form organized patterns. In the capillary regime, the  $\gamma$  is the dominant restoring force and opposes the formation of surface fluctuations that increase the surface area. The application of a sufficiently strong  $E_f$  to polymer–air or polymer–polymer interface overcomes the surface tension and results in electrohydrodynamic (EHD) instability. The EHD model, that is the basis of the work described in this study, was reported by Schaffer et al. [6, 14] who introduced this electrostatic technique based on an instability which develops in (perfect) dielectric viscous polymer in the presence of an electric field. The generic experimental approach and typical experimental results are shown in Fig. 2.6.

### 2.3.2 EHD Patterning Induced by a Homogeneous Electric Field

A polymer when heated above its  $T_g$ , begins to flow as a viscous liquid. Consequently, applying an electric field normal to the initially homogeneous (Fig. 2.6a) interface between two dielectric materials with different dielectric constants yields the destabilizing interfacial  $p_{el}$  which overcomes the intrinsic stabilization of the  $\gamma$ , and couples to the omnipresent part of the capillary wave spectrum, amplifying surface instabilities with a characteristic wavelength,  $\lambda_{max}$  (Fig. 2.6b). A fluid flow with velocity  $v$  during the amplification of the initial capillary film undulations leads

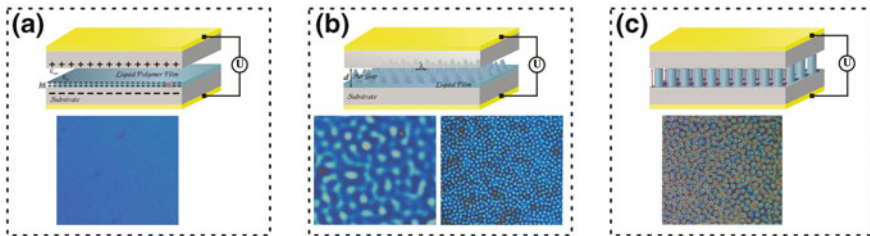


**Fig. 2.6** Representative experimental set-up with an evolving EHD instability of a polymer film under a laterally homogeneous electric field and the corresponding optical micrographs of the EHD pattern formation. **a** Thin polymer film ( $h \approx 100$  nm) deposited on a bottom electrode is opposed by a second planar electrode at distance  $d$  and liquefied at  $T > T_g$  with a voltage  $U$  applied between two electrodes. Small  $d$  generates high  $E_f$  ( $\sim 10^8$  V/m). This results in the amplification of a surface undulation with a characteristic wavelength  $\lambda$  (**b**), which leads to the formation of *hexagonally ordered columns* (**c**). The origin of the destabilizing electrostatic pressure is a result of the electric field which causes the energetically unfavourable build-up of displacement charges at the dielectric interface (**a**), and the alignment of the dielectric interface parallel to the electric field lines (**c**) lowers the electrostatic energy

to a lateral redistribution of the polymer from surrounding thinning regions. These further pinned to the top electrode and detach from the surrounding polymer film by draining the liquid bridge that connects them with the unruptured polymer film. This results in the rearrangement to the energetically favorable configuration of the liquid polymer characterized by an array of pillars with a hexagonal symmetry (Fig. 2.6c) which minimizes the repulsion of the polarized undulations minima and maxima. An inter-pillar distance  $\lambda$  is equal to the initially dominant and amplified capillary wavelength, and is determined by the field strength and the polymer surface tension. The pillars diameter is a function of the initial film thickness.

### 2.3.3 EHD Lithography Induced by a Laterally Varying Electric Field

The intrinsic length scale of EHD instabilities in thin liquid films is on the order of micrometres. It is possible to decrease the length scale to technologically interesting feature sizes by imposing a laterally heterogeneous field variations smaller than the intrinsic wavelength. This can be accomplished by using a topographically structured upper electrode. For an applied electric field, the topographic pattern is an equipotential surface. The variation in the inter-electrode spacing  $d$  therefore results in a lateral inhomogeneous field.

When a laterally varying electric field is applied to the capacitor device, the instability is focused in the direction of the highest electric field (Fig. 2.7b). Since,

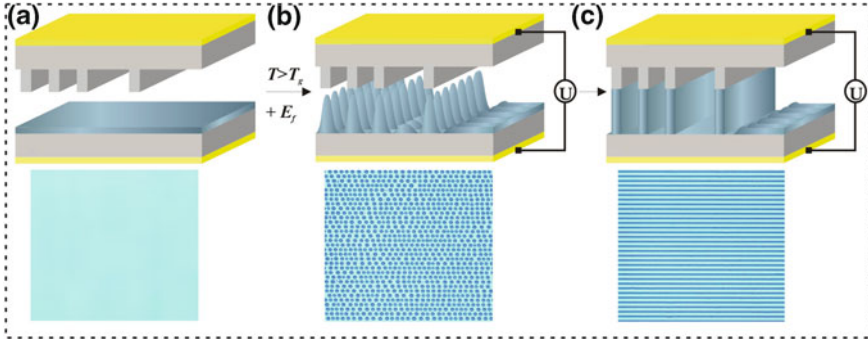


**Fig. 2.7** Top Schematic of experimental device during the EHD lithography process under a laterally heterogeneous electric field. **a** A structured upper plate creates a heterogeneous force field focusing the instability towards the protruding structures **(b)**. In **(c)** a positive replica of the master pattern is transferred into the polymer. In unstructured regions, the film remains stable on a much longer timer scale. *Bottom* Optical micrographs of the pattern replication of a line grating, imaged after immobilization of the thin film and removal of the master electrode: **a** Initial capillary plugs spanning the substrate and protruding lines; **b** increasing coalescence of the capillary plugs; and **c** final replicated grating

$p_{el} \propto 1/d^2$  (Eq. 2.31) the electrostatic pressure is much stronger for smaller electrode distances, pattern replication of topographically structured upper electrode proceeds at a shorter time scale than the regular EHD structure formation. The instability is guided towards the protruding patterns of the top mask, and the liquid polymer is drawn towards these protrusions, forming positive replica (Fig. 2.7c). A successful pattern replication requires harmonizing the length scale of the master pattern and of the instability characteristic wavelength.

This EHD lithographic technique harnesses the initial film instability to replicate a wide range of patterns with high-fidelity and nanometric lateral length scales.

## References

1. Ruckenstein, E., & Jain, R. K. (1974). Spontaneous rupture of thin liquid-films. *Journal of the Chemical Society-Faraday Transactions II*, 70, 132–147.
2. Verma, R., Sharma, A., Kargupta, K., & Bhaumik, J. (2005). Electric field induced instability and pattern formation in thin liquid films. *Langmuir*, 21(8), 3710–3721.
3. Wyart, F. B., Martin, P., & Redon, C. (1993). Liquid–liquid dewetting. *Langmuir*, 9(12), 3682–3690.
4. Bischof, J., Scherer, D., Herminghaus, S., & Leiderer, P. (1996). Dewetting modes of thin metallic films: Nucleation of holes and spinodal dewetting. *Physical Review Letters*, 77(8), 1536–1539.
5. Higgins, A. M., & Jones, R. A. L. (2000). Anisotropic spinodal dewetting as a route to self-assembly of patterned surfaces. *Nature*, 404(6777), 476–478.
6. Schaffer, E. (2001). Instabilities in thin polymer films: structure formation and pattern transfer. Ph.D. thesis. <http://www.ub.uni-konstanz.de/kops/volltexte/2002/779/>.
7. Schaffer, E., Harkema, S., Roerdink, M., Blossey, R., & Steiner, U. (2003). Thermomechanical lithography: pattern replication using a temperature gradient driven instability. *Advanced Materials*, 15(6), 514–517.
8. Seemann, R., Herminghaus, S., & Jacobs, K. (2001). Dewetting patterns and molecular forces: a reconciliation. *Physical Review Letters*, 86(24), 5534–5537.
9. Landau, L. D., & Lifshitz, E. M. (1959). *Fluid mechanics*. London: Pergamon Press.
10. Oron, A., Davis, S. H., & George Bankoff, S. (1997). Long-scale evolution of thin liquid films. *Reviews of Modern Physics*, 69(3), 931–980.
11. Tabor, D., & Winterton, R. H. S. (1969). The direct measurement of normal and retarded van der Waals forces. *Proceeding of the Royal Society A*, 312, 435–450.
12. Lin, Z. Q., Kerle, T., Baker, S. M., Hoagland, D. A., Schaffer, E., Steiner, U., et al. (2001). Electric field induced instabilities at liquid/liquid interfaces. *Journal of Chemical Physics*, 114(5), 2377–2381.
13. Schaffer, E., Thurn-Albrecht, T., Russell, T. P., & Steiner, U. (2001). Electrohydrodynamic instabilities in polymer films. *Europhysics Letters*, 53(4), 518–524.
14. Schaffer, E., Thurn-Albrecht, T., Russell, T. P., & Steiner, U. (2000). Electrically induced structure formation and pattern transfer. *Nature*, 403(6772), 874–877.
15. Pease, L. F., & Russel, W. B. (2003). Electrostatically induced submicron patterning of thin perfect and leaky dielectric films: a generalized linear stability analysis. *Journal of Chemical Physics*, 118(8), 3790–3803.
16. Pease, L. F., & Russel, W. B. (2002). Linear stability analysis of thin leaky dielectric films subjected to electric fields. *Journal of Non-Newtonian Fluid Mechanics*, 102(2), 233–250.
17. Harkema, S. (2006). Capillary instabilities in thin polymer films. Ph.D. thesis. <http://irs.ub.rug.nl/ppn/291147801>.

18. Swan, J. W. (1897). Stress and other effects produced in resin and in a viscid compound of resin and oil by electrification. *Proceedings of the Royal Society*, 62, 38–46.
19. Frenkel, J. (1935). On tonks theory of liquid surface rupture by a uniform electric field. *Physikalische zeitschrift der Sowjetunion*, 8, 675–679.
20. Tonks, L. (1935). A theory of liquid surface rupture by a uniform electric field. *Physical Review*, 48, 562–568.
21. Melcher, J. R. (1963). *Field-coupled surface waves*. Cambridge: MIT Press.
22. Melcher, J. R. (1961). Electrohydrodynamic and magnetohydrodynamic surface waves and instabilities. *Physics of Fluids*, 4, 1348–1354.
23. Reynolds, M. (1965). Stability of electrostatically supported fluid column. *Physics of Fluids*, 8, 161–170.
24. Taylor, G. I., & Mcewan, A. D. (1965). The stability of horizontal fluid interface in a vertical electric field. *The Journal of Fluid Mechanics*, 22, 1–15.

Electrohydrodynamic Patterning of Functional Materials

Oppenheimer, P.G.

2013, XVIII, 137 p. 47 illus., 39 illus. in color., Hardcover

ISBN: 978-3-319-00782-3